ISSN 1070-3284, Russian Journal of Coordination Chemistry, 2024, Vol. 50, No. 7, pp. 492–499. © Pleiades Publishing, Ltd., 2024.

Methylsulfate Complex $(Bu_4N)_2[Mo_6I_8(O_3SOCH_3)_6]$: Synthesis, Structure, Lability of Ligands, and Phosphorescence

M. A. Mikhaylov[a, *], T. S. Sukhikh[a], D. G. Sheven'[a], A. S. Berezin[a], M. N. Sokolov[a, b], and N. B. Kompan'kov[a]

[a] *Nikolaev Institute of Inorganic Chemistry, Siberian Branch, Russian Academy of Sciences, Novosibirsk, Russia*

[b] *Novosibirsk State University, Novosibirsk, Russia*

**e-mail: mikhajlovmaks@yandex.ru*

Received February 7, 2024; revised March 3, 2024; accepted March 6, 2024

Abstract—New methylsulfate complex $(Bu_4N)_2[Mo_6I_8(O_3SOCH_3)_6]$ (**I**) is synthesized by the reaction of $(Bu_4N)_2[Mo_6I_8(C{\equiv}C{-}C(O)OCH_3)_6]$ with dimethyl sulfate $(CH_3)_2SO_4$. According to the XRD data, the molybdenum atoms are coordinated by the monodentate methylsulfate ligands. In a DMSO solution, the complex undergoes solvolysis accompanied by the complete substitution of the methylsulfate ligands by the solvent molecules. A powder sample of cluster **I** luminesces (phosphorescence) with the emission maximum at a wavelength of 620 nm (77 K). Increasing temperature to 300 K results in the shift of the emission maximum to 650 nm and a decrease in the integral intensity by 1.6 times.

Keywords: clusters, molybdenum, methyl sulfate, crystal structure, luminescence properties, solvolysis

DOI: 10.1134/S1070328424600190

INTRODUCTION

Octahedral iodide clusters of molybdenum and tungsten $[M_6I_8L_6]$ represent a new class of materials with strong emission. When excited with light at the wavelengths in the near-UV and IR (to ~470 nm) ranges, $[M_6I_8L_6]$ undergo transitions to the long-lived triplet states followed by the emission of red phosphorescence and transition to the ground (singlet) state [1–5]. The phosphorescence is deactivated in the presence of molecular oxygen due to singlet oxygen formation in a high yield. Owing to the capability of photogenerating singlet oxygen, the $[M_6I_8L_6]$ clusters and related materials have photoinduced cytotoxicity and bactericidal effect. The universal procedures that make it possible to prepare compounds with specified compositions and properties depending on ligand L have been developed to date [1, 6]. High quantum yields and long emission times are the common property of the $(Bu_4N)_2[Mo_6I_8L_6]$ clusters with terminal ligands: anions of strong oxo acids L, such as sulfonates ($PhSO_3^-$, p-$CH_3C_6H_4SO_3^-$) [7], phosphinates ($R_2PO_2^-$) [8, 9], fluorinated carboxylates (R_fCOO^-) [10, 11], and nitrates (NO_3^-) [12]. A similar effect could be expected for the coordination of methyl sulfate ($CH_3OSO_3^-$), since pK_a of methylsulfonic acid CH_3OSO_3H (–3.4 to –3.6) is intermediate between pK_a for CF_3SO_3H (–5.1 to –5.9) and that for aromatic sulfonic acids $PhSO_3H$ (–2.8) and p-$CH_3C_6H_4SO_3H$ (–2.7) [13]. It should be mentioned that alkyl- and arylsulfonic acids are very rarely used as ligands, since their anions are considered as weakly coordinating. For instance, easily available 1-ethyl-3-methylimidazolium ethyl sulfate is considered as the cheapest ionic liquid with the noncoordinating anion [14]. A few complexes with methyl- and ethylsulfate ligands are presently known in which alkyl sulfate plays the role of a coordinated counterion in the heteroleptic cationic complexes with neutral ligands [15–24]. Examples of the coordination of metallocenters by alkyl sulfates only are unknown.

In this work, we report the first complex $(Bu_4N)_2[Mo_6I_8(O_3SOCH_3)_6]$ containing only alkylsulfate terminal ligands, which was synthesized by the treatment of the κ^1-C-methylpropiolate complex $(Bu_4N)_2[Mo_6I_8(C{\equiv}C{-}C(O)OCH_3)_6]$ with dimethyl sulfate.

EXPERIMENTAL

Complex $(Bu_4N)_2[Mo_6I_8(C{\equiv}C{-}C(O)OCH_3)_6]$ was synthesized according to a published procedure [25]. Organic solvents were purified using standard procedures. IR spectra were recorded on a SCIMITAR FTS 2000 spectrometer (4000–400 cm^{-1}). Elemental analysis was conducted at the Analytical Laboratory of the Nikolaev Institute of Inorganic Chemistry (Siberian Branch, Russian Academy of Sciences) on a Euro EA

3000 CHNS analyzer. ^{1}H NMR spectra were recorded at 500 MHz on a Bruker Avance 500 plus spectrometer. Mass spectrometry data were obtained on a liquid chromatograph combined with mass spectrometer (LC-MS) (6130 Quadrupole MS, 1260 infinity LC (Agilent)). An LC-MS analysis was carried out in a mass range of 350–3000 amu for both positively and negatively charged ions in the SCAN mode. Electrospray was used as the ionization source (ESI). A gaseous nitrogen flow served as the drying agent at a temperature of 350°C with a flow rate of 7 L/min, a pressure on the sprayer (nitrogen) of 60 psi, and a voltage on the capillary of 4000 V. The voltage on the fragmentor was zero in all experiments in order to retain weakly bound forms in the mass spectra. A solution of the studied compound (5 μL) in deuterated acetonitrile with a concentration of ~10^{-4} g/mL was introduced into the mobile phase (acetonitrile, special purity grade) with a flow rate of 0.4 mL/min, sprayed, and ionized. The experimental peaks were compared with the calculated values, including those for the isotope distribution. The Molecular Weight Calculator program (by Matthew Monroe) was used for calculations.

Corrected luminescence spectra were recorded on a Fluorolog 3 spectrometer (Horiba Jobin Yvon) equipped with a PC177CE-010 cooled module for photon registration with an R2658 photomultiplier, two double monochromators operating via the Cherney–Turney scheme, a continuous operation xenon lamp (450 W), and a flash xenon lamp (50 W). The luminescence quantum yield was detected under aerated conditions using a Quanta-φ accessory. The temperature dependences were obtained using Optistat-DN accessory.

Synthesis of $(Bu_4N)_2[Mo_6I_8(O_3SOCH_3)_6]$ (I). Dimethyl sulfate $(CH_3)_2SO_4$ (10 mL) was added to a powder of $(Bu_4N)_2[Mo_6I_8(C{\equiv}C{-}C(O)OCH_3)_6]$ (0.20 g, 0.077 mmol) placed in a glass vial with a crewed plastic cap, and a magnetic stirring element was placed in the vial. The reaction mixture in the closed vial was magnetically stirred for 3 days with heating at 100°C, and the vial was covered with an aluminum foil to prevent heat losses. The blurred reaction solution was centrifuged and poured to a conic flask, and the product was precipitated by the addition of diethyl ether followed by holding the mixture in a freezer. The solution was decanted from the formed oil, which was dissolved in acetonitrile (7 mL). Complex **I** as an orange polycrystalline powder was precipitated from the formed solution with diethyl ether. The precipitate was filtered off on a glass filter, washed with diethyl ether, and dried on the filter. The yield was 130 mg (61%).

IR (KBr; ν, cm^{-1}): 2963 m, 2876 m, 1472 m, 1462 m, 1383 w, 1317 sh s, 1304 s, 1182 sh s, 1169 s, 1026 s, 976 s, 928 sh m, 878 m, 831 w, 777 s, 735 sh m, 617 m, 584 m, 542 m, 436 m. MS (ESI, CH_3CN, *m/z*): maximum-intensity peaks in the found isotope distributions at 1129.7 and 2500.9; calculated positions of maxima 1129.8 (for $[Mo_6I_8(O_3SOCH_3)_6]^{2-}$) and 2500.8 (for $\{(Bu_4N)[Mo_6I_8(O_3SOCH_3)_6]\}^-$). ^{1}H NMR (DMSO-$d_6$; δ, ppm, normalized to 24 protons of CH_3 groups of Bu_4N^+): 3.62 (s, 18 H, CH_3 groups of methyl sulfate).

For $C_{38}H_{90}N_2O_{24}S_6I_8Mo_6$				
Anal. calcd., %	C, 16.6	H, 3.3	N, 1.02	S, 6.9
Found, %	C, 16.4	H, 3.3	N, 1.02	S, 6.8

Single crystals suitable for XRD were prepared by the diffusion of diethyl ether vapors to a solution of the complex in dichloromethane.

XRD of a single crystal of complex **I** was conducted at the Center for Collective Use of the Nikolaev Institute of Inorganic Chemistry (Siberian Branch, Russian Academy of Sciences) on a Bruker D8 Venture diffractometer with a CMOS PHOTON III detector and an IμS 3.0 microfocus source (MoK_α radiation (λ = 0.71073 Å), Montel focusing mirrors). The crystal structure was solved using the SHELXT program [26] and refined using the SHELXL programs [27] with the OLEX2 graphical interface [28]. Atomic shift parameters for non-hydrogen atoms were refined anisotropically. Hydrogen atoms were revealed geometrically and refined by the riding model. Selected interatomic distances in the structure of complex **I** are given in Table 1.

The crystallographic characteristics and structure refinement details for $C_{38}H_{90}N_2O_{24}S_6I_8Mo_6$ (FW = 2742.31 g/mol) are as follows: space group $P\bar{1}$, a = 11.8067(6), b = 13.0653(6), c = 13.9005(7) Å, α = 106.648(2)°, β = 109.815(2)°, γ = 97.882(2)°, V = 1866.34(16) Å^3, Z = 1, T = 150(2) K, μ(MoK_α) = 4.519 mm^{-1}, ρ_{calc} = 2.440 g/cm^3, 22490 measured reflections (4.374° ≤ 2θ ≤ 54.264°), 8191 independent reflections (R_{int} = 0.0337, R_σ = 0.0409); R_1 = 0.0334 ($I > 2\sigma(I)$), wR_2 = 0.0766 (all data), $\Delta\rho_{max}/\Delta\rho_{min}$ = 1.49/–0.96 e/Å^3.

The structure was deposited with the Cambridge Crystallographic Data Centre (CIF file CCDC no. 2312454; deposit@ccdc.cam.ac.uk or http://www.ccdc.cam.ac.uk).

RESULTS AND DISCUSSION

In this work, we attempted to alkylate the κ^1-C-methylpropiolate complex $(Bu_4N)_2[Mo_6I_8(C{\equiv}C{-}C(O)OCH_3)_6]$ with dimethyl sulfate. It was assumed that the carbonyl oxygen atom of the ligand is subjected to alkylation to form the vinylidene ligand $C{=}C{=}C(OCH_3)_2$. However, the end product was the methylsulfate complex $(Bu_4N)_2[Mo_6I_8(O_3SOCH_3)_6]$ (**I**). Its formation can be explained if assuming the

Table 1. Bond lengths Mo–Mo, Mo–I, and Mo–O in the structure of compound **I***

Bond	*d*, Å	Bond	*d*, Å
Mo(1)–Mo(2)	2.6613(6)	$I(2)^1$–$Mo(2)^1$	2.7716(5)
$Mo(1)^1$–$Mo(2)^1$	2.6613(6)	I(2)–Mo(3)	2.7773(5)
Mo(1)–Mo(3)	2.6509(6)	$I(2)^1$–$Mo(3)^1$	2.7773(5)
$Mo(1)^1$–$Mo(3)^1$	2.6509(6)	I(3)–Mo(1)	2.7807(5)
Mo(1)–$Mo(2)^1$	2.6558(6)	$I(3)^1$–$Mo(1)^1$	2.7807(5)
$Mo(1)^1$–Mo(2)	2.6558(6)	I(3)–Mo(2)	2.7716(5)
Mo(1)–$Mo(3)^1$	2.6542(6)	$I(3)^1$–$Mo(2)^1$	2.7716(5)
$Mo(1)^1$–Mo(3)	2.6542(6)	I(3)–$Mo(3)^1$	2.7788(6)
Mo(2)–Mo(3)	2.6630(6)	$I(3)^1$–Mo(3)	2.7788(6)
$Mo(2)^1$–$Mo(3)^1$	2.6630(6)	I(4)–Mo(1)	2.7796(5)
Mo(2)–$Mo(3)^1$	2.6622(6)	$I(4)^1$–$Mo(1)^1$	2.7796(5)
$Mo(2)^1$–Mo(3)	2.6622(6)	I(4)–$Mo(2)^1$	2.7863(5)
I(1)–Mo(1)	2.7806(5)	$I(4)^1$–Mo(2)	2.7863(5)
$I(1)^1$–$Mo(1)^1$	2.7806(5)	I(4)–Mo(3)	2.7825(5)
I(1)–Mo(2)	2.7638(5)	$I(4)^1$–$Mo(3)^1$	2.7825(5)
$I(1)^1$–$Mo(2)^1$	2.7638(5)	Mo(1)–O(1)	2.126(4)
I(1)–Mo(3)	2.7565(6)	$Mo(1)^1$–$O(1)^1$	2.126(4)
$I(1)^1$–$Mo(3)^1$	2.7565(6)	Mo(2)–O(9)	2.157(3)
I(2)–$Mo(1)^1$	2.7724(5)	$Mo(2)^1$–$O(9)^1$	2.157(3)
$I(2)^1$–Mo(1)	2.7724(5)	Mo(3)–O(5)	2.140(3)
I(2)–Mo(2)	2.7716(5)	$Mo(3)^1$–$O(5)^1$	2.140(3)

Symmetry codes: ^{1} $1-x$, $1-y$, $1-z$.

alkylation of the methylpropiolate ligand at the carbon atom with the formation of the more stable product $CH_3C{\equiv}C{-}C(O)OCH_3$, which leaves the coordination sphere. The methylsulfate anion $CH_3OSO_3^-$ formed due to the methyl group transfer from dimethyl sulfate coordinates via the κ^1-O-type monodentate mode to the cluster core. Remarkably, the methylation does not occur under mild conditions (CH_2Cl_2, nitrobenzene, $(CH_3)_2SO_4$, room temperature), and the signals from the initial methylpropiolate complex $[Mo_6I_8(C{\equiv}C{-}C(O)OCH_3)_6]^{2-}$ are detected in the mass spectrum (in the negative *m/z* range). If the methylation is carried out at elevated temperature (90°C and higher) in nitrobenzene, then the reaction does not occur to the end even at a 48-fold molar excess of $(CH_3)_2SO_4$ per mole of $(Bu_4N)_2[Mo_6I_8(C{\equiv}C{-}C(O)OCH_3)_6]$. Therefore, the best method for the reaction is the use of $(CH_3)_2SO_4$ simultaneously as the solution and reactant, which warrants the shift of the reaction equilibrium to the right with the formation of $(Bu_4N)_2[Mo_6I_8(O_3SOCH_3)_6]$ as the single product.

As far as we know, the $[Mo_6I_8(O_3SOCH_3)_6]^{2-}$ cluster is the first example of the alkylsulfate complexes in which ligands of this type occupy all terminal positions. It has recently been shown [29] that the attempt to synthesize the corresponding vinylidene complex by the methylation of the phenylacetylenide ligand in $[Re_6Se_8(PEt_3)_5(C{\equiv}C{-}Ph)](SbF_6)$ with methyl triflate also resulted in the elimination of the alkynyl ligand and the methylsulfate complex $[Re_6Se_8(PEt_3)_5(O_3SOCH_3)](SbF_6)$ turned out to be the end product.

Target compound **I** in the powdered form is prepared by precipitation from the reaction solution in $(CH_3)_2SO_4$ by the addition of diethyl ether to the solution. If necessary, the substance can repeatedly by precipitated from CH_2Cl_2 also by the addition of Et_2O.

The fragment of the crystalline lattice is shown in Fig. 1a. The crystal of complex **I** contains no solvate molecules and specific interactions between the particles, and the space is uniformly filled with the electrostatically interacting cluster anions and tetrabutylammonium cations. Each molybdenum atom is coordinated via the monodentate mode by six ligands through the oxygen atom of the methylsulfate ligand,

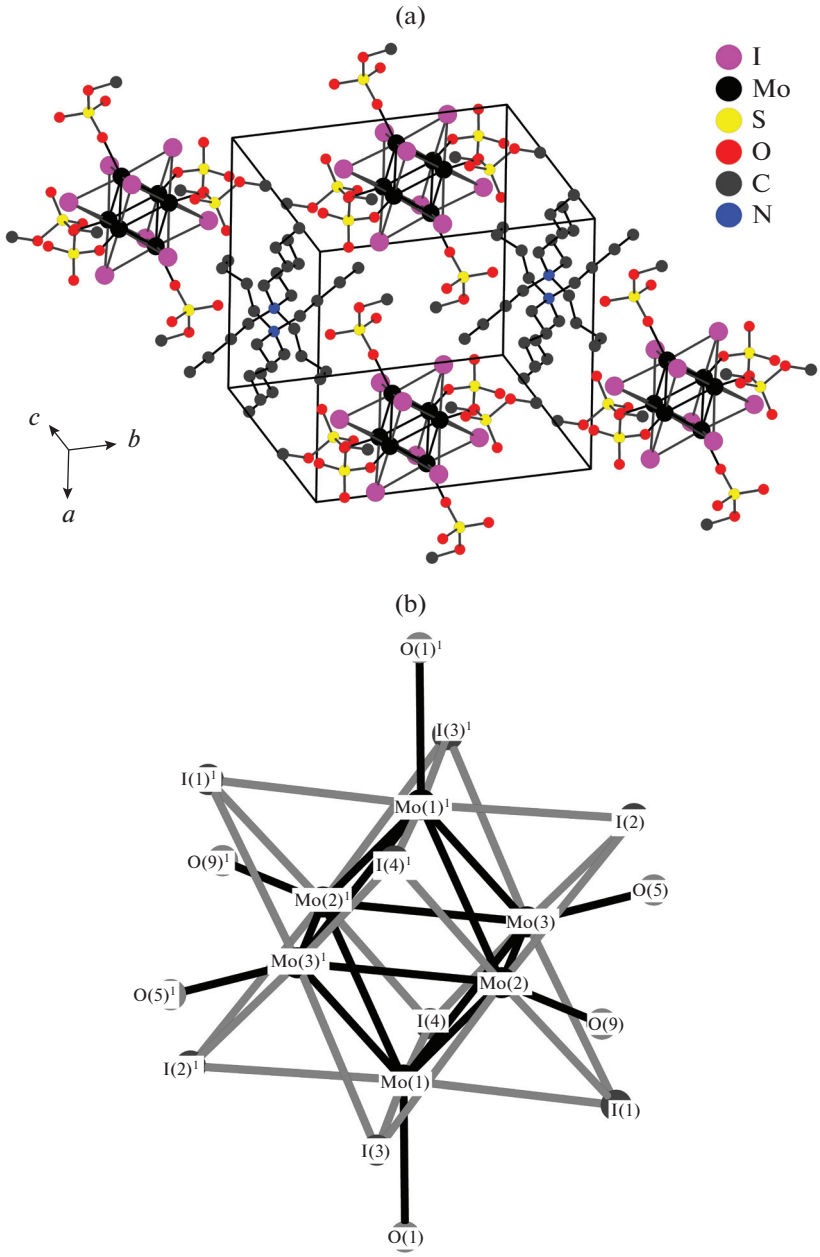

Fig. 1. (a) Fragment of the crystal structure of cluster **I** (hydrogen atoms are omitted) and (b) the fragment of the cluster anion in complex **I** (crystallographically equivalent Mo, I, and O atoms are given in parentheses; the superscript at the parentheses designates the corresponding centrosymmetric atom).

which is the typical coordination mode of ligands in complexes of the $[\{M_6X_8\}L_6]$ type (M = Mo, X = halogen) regardless of the number and type of donor atoms of the ligands. The average Mo–O distance in complex **I** is 2.14 Å, which is comparable with the average Mo–O distances (2.13 Å) in the tosylate complex $(Bu_4N)_2[Mo_6I_8(O_3SC_6H_4CH_3)_6]\cdot 2Et_2O\cdot 2CH_3CN$ [30], with the average Mo–O distances (2.11 Å) in solvates of the tosylate chloride complexes $(Bu_4N)_2[Mo_6Cl_8(O_3SC_6H_4CH_3)_6]\cdot 2CH_3CN$ and $(Bu_4N)_2[Mo_6Cl_8(O_3SC_6H_4CH_3)_6]\cdot CH_2Cl_2$ [31], and with the average Mo–O distances (2.17 Å) in the triflate complex $(Bu_4N)_2[Mo_6I_8(O_3SCF_3)_6]\cdot CH_2Cl_2$ [4]. The Mo–Mo and Mo–I distances in complex **I** are given in Table 1 and are characteristic distances for cluster cores of the $\{Mo_6I_8\}^{4+}$ type [30, 32, 33] (Fig. 1b).

Such ligands as triflate $CF_3SO_3^-$ and tosylate (*p*-toluenesulfonate, Pts) $CH_3C_6H_4SO_3^-$ are known to be labile and, hence, a resembling lability should be expected for the methylsulfonate ligands in solutions

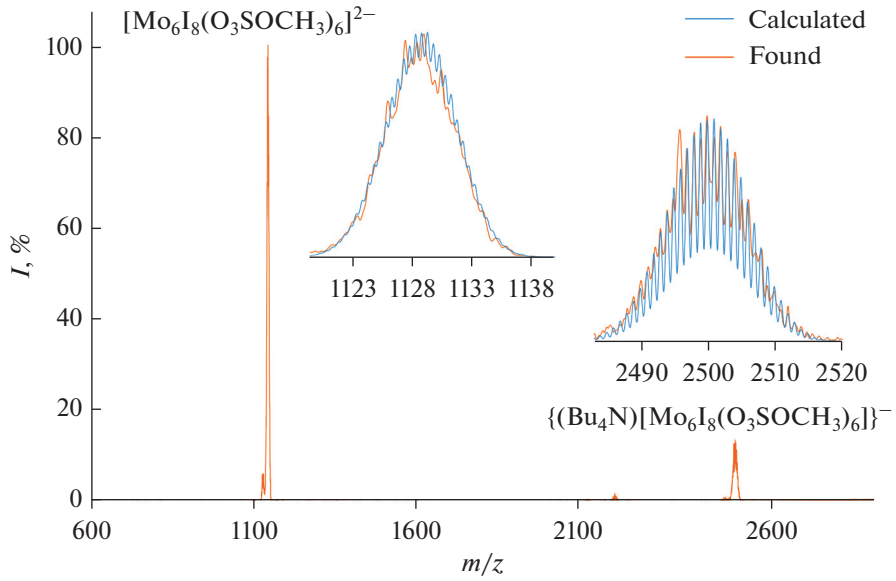

Fig. 2. Found and calculated isotope distributions in the negative m/z range corresponding to $[Mo_6I_8(O_3SOCH_3)_6]^{2-}$ and $\{(Bu_4N)[Mo_6I_8(O_3SOCH_3)_6]\}^-$.

of complex **I** with respect to donor solvents. No immediate substitution of methylsulfate ligands occurred in acetonitrile, and the mass spectrum (ESI) of an acetonitrile solution of complex **I** exhibits (in the negative m/z range) signals with maxima in the isotope distributions at 1129.7 and 2500.9 corresponding to the $[Mo_6I_8(O_3SOCH_3)_6]^{2-}$ complex and $\{(Bu_4N)[Mo_6I_8(O_3SOCH_3)_6]\}^-$ ionic associate. The superposition of the found and calculated isotope distributions for these anions is shown in Fig. 2.

^{1}H NMR spectroscopy providing a series of spectra at various temperatures and holding times was used for the quantitative estimation of the degree of solvolysis of $(Bu_4N)_2[Mo_6I_8(O_3SOCH_3)_6]$ (**I**) in DMSO-d_6. A solution of complex **I** at room temperature mainly contains unsubstituted $(Bu_4N)_2[Mo_6I_8(O_3SOCH_3)_6]$. The integral ratio of signals from the protons of the ligands (singlet, δ = 3.62 ppm) and from the methyl protons of the tetrabutylammonium cations (triplet, δ = 1.08 ppm) is 0.14/0.10 = 1.4 ≈ 24/18 and corresponds to six methylsulfate ligands (18 protons) and two tetrabutylammonium cations (24 methyl protons) in a solution of complex **I** in DMSO-d_6. The substitution of the methylsulfate ligands starts at 40°C and higher. A new signal appears above 40°C (δ = 3.38 ppm) corresponding to the protons of free methyl sulfate (Fig. 3, signals of $CH_3OSO_3^-$ at various T are marked with orange oval), and the intensity of this signal first increases with further heating (reaching a maximum at 60°C) and then decreases because of the hydrolysis of free triflate anions with water traces in the solvent: $CH_3OSO_3^- + H_2O = HSO_4^- + CH_3OH$. Correspondingly, the intensity of the signal from the protons of the methyl group of methanol (δ = 3.22 ppm), which appears at T = 60°C, increases with hydrolysis. This signal (marked with red oval inside rectangle in Fig. 3) is superimposed with the multiplet of the protons of the methylene groups ($-CH_2-$) of the tetrabutylammonium cations (signals are marked with rectangles). The substitution of the methylsulfate ligands by DMSO nearly completely comes to the end at 60°C within 45 min. As in the case of solvolysis of tosylate ligands $(Bu_4N)_2[M_6I_8(O_3SC_6H_4CH_3)_6]$ (M = Mo, W) in a solution of DMSO-d_6, the chemical shifts from the protons of the coordinated ligands are insensitive to the degree of substitution, and only the ratio of integral intensities of the signals (from the protons of coordinated ions L (in $[M_6I_8L_{6-x}(DMSO\text{-}d_6)_x]^{-(2-x)}$ (M = Mo, W) and uncoordinated ions (L = $CH_3C_6H_4SO_3^-$, $CH_3OSO_3^-$) changes [30]. The intensity of the unsplit signal with the center at δ = 3.62 ppm (from the protons of the coordinated methylsulfate ligands) decreases with their substitution by DMSO-d_6 molecules: the equal amounts of free and coordinated methylsulfate ions are observed in the solution when reaching 60°C, and the signal from the protons of the coordinated ligands disappears almost completely as a solution of complex **I** is further held at 60°C. When a temperature of 80°C is reached and the sample of complex **I** is held further at this temperature for 45 min, 67% free methyl sulfate are hydrolyzed. No backward coordination of the methylsulfate ligands occurs with cooling the solutions to room temperature.

It can be asserted on the basis of the data obtained that the methylsulfate ligands of the $\{Mo_6I_8\}$ cluster

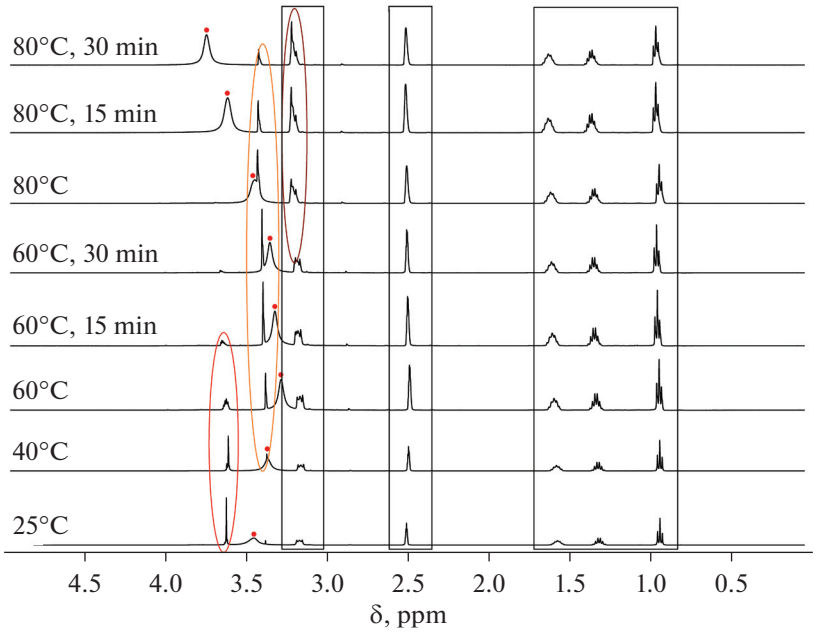

Fig. 3. ^{1}H NMR spectra of complex **I** in DMSO-d_6 at various temperatures. Chemical shifts of signals from the protons of the Bu_4N^+ cation and DMSO (2.5 ppm) are marked with rectangles, those from the methyl protons of the methanol molecules are marked with red oval inside rectangle, orange oval indicates chemical shifts from the protons of the free methylsulfate anions, red oval indicates chemical shifts from the protons of the coordinated methylsulfate anions, and the migrating (in a range of 3.31–3.74 ppm) broadened signal marked with red point is assigned to the protons of H_2O.

are more labile in solvolysis than the tosylate ligands: the solvolysis of the latter, $(Bu_4N)_2[Mo_6I_8(O_3SC_6H_4CH_3)_6]$, in DMSO results in the coexistence of the cationic complexes $[Mo_6I_8(O_3SC_6H_4CH_3)(DMSO)_5]^{3+}$ with a minor fraction of $[Mo_6I_8(DMSO)_6]^{4+}$ after holding the solution at 100°C for 14.5 h, whereas the substitution of the methylsulfate ligands is complete with the formation of the dimethylsulfoxide complex [34].

The powder sample of cluster **I** demonstrates the long-lived luminescence (phosphorescence) with a maximum at 620 nm at 77 K. Increasing temperature to 300 K results in the red shift of the emission maximum to 650 nm with a simultaneous decrease in the integral intensity by 1.6 times (Fig. 4). The excitation spectrum at room temperature represents a broad line in a range of 250–600 nm with a maximum at 450 nm and two weakly pronounced additional maxima, whose linewidths decrease with decreasing temperature to 77 K with the simultaneous hypsochromic shift of these maxima to 440, 500, and 575 nm (Fig. 5). The luminescence spectrum of complex **I** cannot satisfactorily be described by one Gauss function in direct energy values. This is related, most likely, to diverse spectrally unresolved luminescence bands. This behavior is characteristic of cluster emitters with the $\{M_6X_8\}$ core, which can undergo transitions from four sublevels of the excited triplet state [35]. At the same time, the observed monoexponential luminescence decay can be explained by averaging rate constants of transitions from different excited sublevels. The luminescence decay is well described by the monoexponential function with the independent luminescence lifetime $\tau = 170$ μs. The temperature dependence of the integral luminescence intensity can be described by the following equation:

$$I(T) = I_0 \Big/ \left(1 + Ce^{-\Delta E/kT}\right),$$

where I_0 is temperature-independent intensity, C is the dimensionless parameter, and ΔE is the activation energy of thermal quenching of luminescence, and $\Delta E = 700$ K (487 cm^{-1}) (Fig. 6). The luminescence quantum yield of complex **I** is 29% at 300 K and excitation at a wavelength of 440 nm. Phosphorescence quenching with oxygen is usually stronger for solution samples than for samples in the solid state, which can be due to the fact that the diffusion of oxygen molecules to luminescent centers in the solid substance is more difficult than that in solutions. For instance, in the case of complexes $(Bu_4N)_2[M_6I_8(CF_3COO)_6]$ (M = Mo, W) dissolved in acetonitrile solutions saturated with air oxygen, luminescence quenching is almost complete, whereas the luminescence quantum yields of pure polycrystalline samples reach 4% (W) and 12% (Mo) [5]. The difference in the sizes of particles (agglomerates) at the macroscopic level (hundreds of micrometers) in the powder samples exerts no effect on the luminescence quenching with air oxygen according to the data of experiments on grinding and

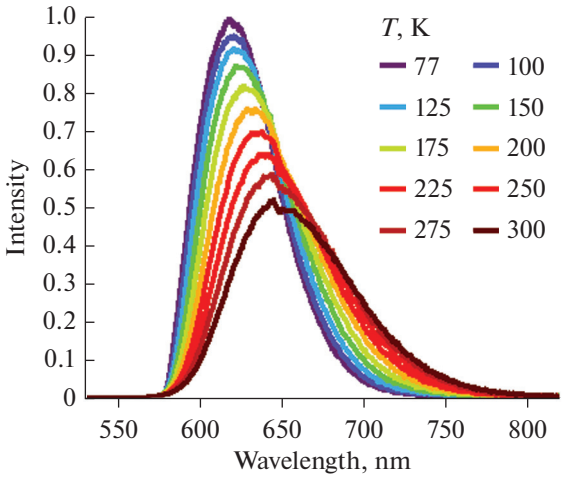

Fig. 4. Temperature dependence of the luminescence of powder sample **I** upon excitation at λ_{ex} = 440 nm.

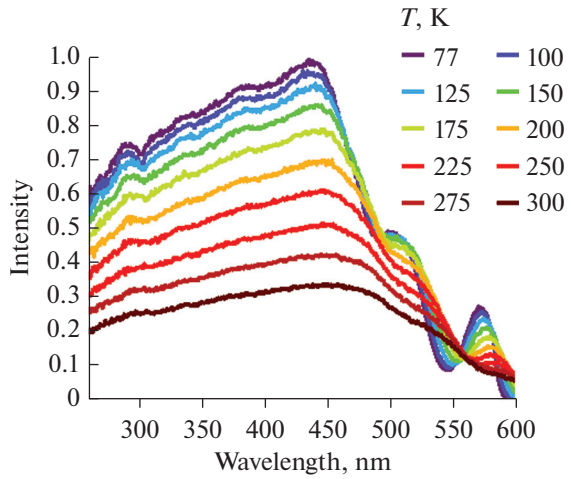

Fig. 5. Temperature dependence of the excitation spectrum of a powder of cluster **I** with the luminescence maximum at λ_{em} = 620 nm.

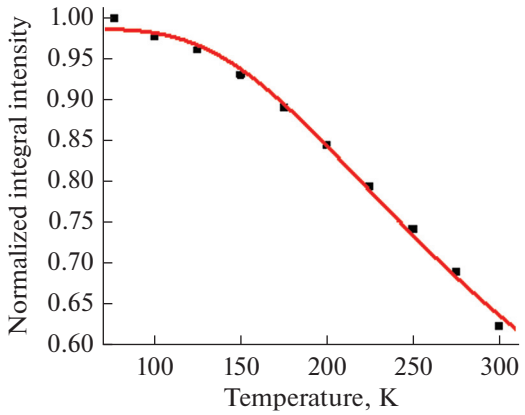

Fig. 6. Temperature dependences of the luminescence intensity of complex **I** upon excitation at λ_{ex} = 440 nm.

checking particle sizes (on a scanning electron microscope) combined with repeated spectroscopic measurements [4].

FUNDING

This work was supported by the Ministry of Science and Higher Education of the Russian Federation, project no. 121031700313-8.

CONFLICT OF INTEREST

The authors of this work declare that they have no conflicts of interest.

REFERENCES

1. Mikhaylov, M.A. and Sokolov, M.N., *Eur. J. Inorg. Chem.*, 2019, vol. 2019, nos. 39–40, p. 4181.
2. Zietlow, T.C., Nocera, D.G., and Gray, H.B., *Inorg. Chem.*, 1986, vol. 25, no. 9, p. 1351.
3. Hummel, T., Ströbele, M., Schmid, D., et al., *Eur. J. Inorg. Chem.*, 2016, vol. 2016, no. 31, p. 4938. https://doi.org/10.1002/ejic.201600926
4. Fuhrmann, A.D., Seyboldt, A., Schank, A., et al., *Eur. J. Inorg. Chem.*, 2017, vol. 2017, no. 37, p. 4259.
5. Riehl, L., Seyboldt, A., Ströbele, M., et al., *Dalton Trans.*, 2016, vol. 45, p. 15500.
6. Vorotnikova, N.A., Vorotnikov, Y.A., and Shestopalov, M.A., *Coord. Chem. Rev.*, 2024, vol. 500, p. 215543. https://doi.org/10.1016/j.ccr.2023.215543
7. Efremova, O.A., Vorotnikov, Y.A., Brylev, K.A., et al., *Dalton Trans.*, 2016, vol. 39, p. 15427.
8. Mironova, A.D., Mikhajlov, M.A., Sukhikh, T.S., et al., *Z. Anorg. Allg. Chem.*, 2019, vol. 645, nos. 18–19, p. 1135.
9. Kirakci, K., Demel, J., Hynek, J., et al., *Inorg. Chem.*, 2019, vol. 58, p. 16546.
10. Vorotnikova, N.A., Alekseev, A.Y., Vorotnikov, Y.A., et al., *Mater. Sci. Eng.*, 2019, vol. 105, p. 110.
11. Mikhailov, M.A., Brylev, K.A., Abramov, P.A., et al., *Inorg. Chem.*, 2016, vol. 55, p. 8437.
12. Svezhentseva, E.V., Solovieva, A.O., Vorotnikov, Y.A., et al., *New J. Chem.*, 2017, vol. 41, p. 1670.
13. Stewart, R., *The Proton: Applications to Organic Chemistry,* Elsevier, 1985, vol. 46, p. 9. https://doi.org/10.1016/B978-0-12-670370-2.50006-2
14. Schmeisser, M., Heinemann, F.W., Illner, P., et al., *Inorg. Chem.*, 2011, vol. 50, p. 6685.
15. Blösl, S., Schwarz, W., and Schmidt, A., *Z. Anorg. Allg. Chem.*, 1982, vol. 495, p. 177.
16. Seebacher, J., Mian, J., and Vahrenkamp, H., *Eur. J. Inorg. Chem.*, 2004, vol. 2004, p. 409.
17. Li, Y., Lu, J., Cui, X.B., et al., *Pol. J. Chem.*, 2004, vol. 78, no. 6, p. 779.
18. Belokon', Y.N., Clegg, W., Harrington, R.W., et al., *Inorg. Chem.*, 2008, vol. 47, p. 3801.
19. Song, L. and Iyoda, T., *J. Inorg. Organomet. Polym. Mater.*, 2009, vol. 19, p. 124.

20. Wu, J.Y., Zhong, M.-S., Chiang, M.-H., et al., *Chem.-Eur. J.*, 2016, vol. 22, p. 7238.
21. Orysyk, S.I., Bon, V.V., Pekhnyo, V.I., et al., *Polyhedron*, 2012, vol. 38, p. 15.
22. Vimala, T.M. and Swaminathan, S., *Curr. Sci.*, 1969, vol. 38, p. 362.
23. Chifotides, H.T., Hess, J.S., Angeles-Boza, A.M., et al., *Dalton Trans.*, 2003, p. 4426.
24. Blake, A.J., Hubberstey, P., Suksangpanya, U., and Wilson, C.L., *Dalton Trans.*, 2000, p. 3873. https://doi.org/10.1039/B003427O
25. Sokolov, M.N., Mikhailov, M.A., Brylev, K.A., et al., *Inorg. Chem.*, 2013, vol. 52, p. 12477.
26. Sheldrick, G.M., *Acta Crystallogr., Sect. A: Found. Adv.*, 2015, vol. 71, p. 3. https://doi.org/10.1107/S2053273314026370
27. Sheldrick, G.M., *Acta Crystallogr., Sect. C: Struct. Chem.*, 2015, vol. 71, p. 3. https://doi.org/10.1107/S2053229614024218
28. Dolomanov, O.V., Bourhis, L.J., Gildea, R.J., et al., *J. Appl. Crystallogr.*, 2009, vol. 42, p. 339. https://doi.org/10.1107/S0021889808042726
29. Soto, E., Helmink, K.L., and Chin, C.P., *Organometallics*, 2022, vol. 41, p. 2688.
30. Mikhailov, M.A., Gushchin, A.L., Gallyamov, M.R., et al., *Russ. J. Coord. Chem.*, 2017, vol. 43, p. 172. https://doi.org/10.1134/S107032841702004X
31. Sokolov, M.N., Mikhailov, M.A., Abramov, P.A., and Fedin, V.P., *J. Struct. Chem.*, 2012, vol. 53, no. 1, p. 200.
32. Bruckner, P., Preetz, W., and Punjer, M., *Z. Anorg. Allg. Chem.*, 1997, vol. 623, p. 8.
33. Kirakci, K., Cordier, S., Roisnel, T., et al., *Z. Kristallogr. NCS*, 2005, vol. 220, p. 116.
34. Pronina, E.V., Pozmogova, T.N., Vorotnikov, Y.A., et al., *J. Biol. Inorg. Chem.*, 2022, vol. 27, p. 111. https://doi.org/10.1007/s00775-021-01914-3
35. Mikhailov, M.A., Berezin, A.S., Sukhikh, T.S., et al., *J. Struct. Chem.*, 2021, vol. 62, no. 12, p. 1896.

Translated by E. Yablonskaya